Ecological Modelling 348 (2017) 33–43

Contents lists available at ScienceDirect

Ecological Modelling

journal homepage: www.elsevier.com/locate/ecolmodel

Forest fire spread simulating model using cellular automaton with extreme learning machine

Zhong Zheng [a,b,c], Wei Huang [d,*], Songnian Li [d], Yongnian Zeng [a,c]

[a] School of Geoscience and Info-Physics, Central South University, Changsha 410083, Hunan, China
[b] College of Resources and Environment, Chengdu University of Information Technology, Chengdu 610225, Sichuan, China
[c] Spatial Information Technology and Sustainable Development Research Center, Central South University, Changsha 410083, Hunan, China
[d] Department of Civil Engineering, Ryerson University, Toronto, Ontario M5B 2K3, Canada

ARTICLE INFO

Article history:
Received 15 August 2016
Received in revised form
23 November 2016
Accepted 27 December 2016

Keywords:
Cellular automaton
Machine learning
Forest fire
Simulation

ABSTRACT

The quantitative simulation of forest fire spreading plays an essential role in designing quick risk management and implementing effective suppression policies. As a preferable modelling approach, the cellular automaton (CA) has been used to simulate the complex mechanisms of fire spreading. However, in traditional CA models, comprehensive studies on the physical principles of forest fires are needed to define the local transition rules. Instead of defining transition rules, the Extreme Learning Machine (ELM) was applied in this study. By integrating the ELM with the traditional forest fire CA framework, a new cellular automaton modelling approach was proposed. After that, its performance was validated using data collected from five fires in the west of United States. Results show that the ELM performed well in predicting each cell's igniting probability. The impact of wind velocity on fire spreading pattern can be effectively described by the proposed modelling approach. Furthermore, the validation against actual fire behavior observations shows that its simulation performance is acceptable and in most cases is better than that of the previously reported studies.

1. Introduction

World-widely, forest fire has become one of the most critical natural hazards in recent years (Quintano et al., 2013; Zheng et al., 2016). It can result in enormous damage to ecological environment and serious loss of human life, and destroy economic development (Sun et al., 2013; Chang et al., 2016). There is no doubt that quantifying its spreading process in more systematic and efficient ways will play a critical role in fire risk management and suppression policy implementations (Alexandridis et al., 2011). However, the simulation of spread process has been challenged by the complexity and non-linear nature of forest fire spread system (Encinas et al., 2007; Russo et al., 2014). In this context, a growing number of models e.g., physical and quasi-physical models (Sullivan, 2009a), empirical and quasi-empirical models (Sullivan, 2009b), and simulation and mathematical analogue models (Sullivan, 2009c), have recently been developed to address such challenges (Alexandridis et al., 2008).

quasi-similar

Cellular automaton (CA) is a relatively simple modelling approach, which is compatible with Geographical Information Systems (GIS) (Sullivan, 2009c). Therefore, it has been applied to reproduce the evolution of some natural phenomena, such as lattice gas (Meyer, 1996), epidemic propagation (White et al., 2007), ecological modelling (Hogeweg, 1988), and urban growth (Clarke and Gaydos, 1998). This modelling approach is also commonly used for simulating the forest fire spread since it can simulate more complex mechanisms of forest fire spreading without conducting intensive preliminary studies about its general evolution causes (Rienow and Goetzke, 2015). As a bottom-up modelling approach, it only requires simple transition rules between the local neighboring cells (Alexandridis et al., 2011). This leads to the significant efforts on investigating in the development of these local transition rules in such modelling approaches in the past several years.

The CA framework was first introduced by von Neumann (1966). Its first application of forest fire simulating was carried out by Albinet et al. (1986), which was based on some idealized heat transmission rules between burning and unburned neighboring cells under isotropic conditions. By extending the transition rules of Albinet's modelling approach to anisotropic conditions (e.g., wind and slope), Niessen and Blumen (1988) assigned different ignition probabilities for crown and surface fires. Following these

isotropic-same properties from all the axes

* Corresponding author at. Ryerson University, 350 Victoria Street, Toronto, Ontario M5B 2K3, Canada.
E-mail address: wei1.huang@ryerson.ca (W. Huang).

http://dx.doi.org/10.1016/j.ecolmodel.2016.12.022
0304-3800/

studies, Gonçalves and Diogo (1994) updated the traditional local transition rules of square-lattice CA modelling approach based on Rothermel's equations of fire rate spread, and Trunfio (2004) and Zhang et al. (2004) extended them to the hexagonal-lattice CA Modelling approach. Further, considering fire spread variations in homogeneous and heterogeneous forests, Karafyllidis and Thanailakis (1997) developed some local transition rules of CA modelling approach. To modify the linear front of local transition rules in Karafyllidis and Thanailakis's modelling approach, Hernández Encinas et al. (2007) applied the circular spreading of the fire front when it came from a diagonal cell. After that, Collin et al. (2011) defined the cellular automaton rules from vegetation and flame characteristics based on a physical modelling approach. In addition, for incorporating the effect of fire suppression tactics in CA modelling approach, Alexandridis et al. (2011) made necessary changes in transition rules. More recently, by combining CA framework with Wang's fire physical velocity modelling approach (Wang, 1992), Sun et al. (2013) proposed a more practical mountain fire spread modelling approach at fine scale for the forest areas in Southwest China.

Although above CA modelling approaches can capture the complex development of fire spread patterns, their performance still largely depends on the efficiency and accuracy of human-made local transition rules. This means, in the process of creating these local transition rules, a certain amount of comprehensive studies about the physical principles of forest fire are still needed. Moreover, the parameters required by these physical principles in local rules of these CA modelling approaches were generally obtained from published studies or laboratory experiments. To make local transition rules work better for simulating fire spread in specific areas, more efforts on adjusting parameters also are required.

These issues have also been echoed by the CA-based urban growth studies and great progress has been made to address them (Li and Liu, 2006; Li and Yeh, 2002; Pei et al., 2015; Rienow and Goetzke, 2015). More specifically, for CA-based urban growth modelling approaches, local transition rules can be built by introducing local historic training data and adaptive data-driven learning methods (e.g., logistic regression algorithm, artificial neural network, support vector machine and extreme learning machine). By introducing these methods, it has become easier for researchers to construct a more effective and adaptive CA modelling approach for urban growth studies of a specified area.

This paper proposes a novel cellular automaton modelling approach that integrates the traditional forest fire CA framework with the Extreme Learning Machine (ELM) which is a very popular model for data-driven learning. In this modelling approach, the local evolution rules of fire spreading are created by ELM using local historic training data, which ensures the building of a simple CA modelling approach that can be easily applied without considering the complicated theory of traditional modelling approaches and several physical parameters. The paper is structured as follows. The background of CA modelling approach is introduced in Section 1. Section 2 reviews the recent efforts in the field of data-driven fire spread simulation. Section 3 presents the details of the proposed cellular automaton modelling approach, followed by the study area and data. Section 5 presents results and discussion. Finally, Section 6 provides the conclusion of this study and the work needed to be done further.

2. Background of data-driven fire spread simulation

Coupled with the ability of better exploiting data from real fires, data-driven methods have the potential to improve the accuracy of fire spread simulation (Ntinas et al., 2016). Some effective and advanced data-driven models have therefore been proposed in recent years.

For example, based on the observed evolutions of recent forest fires and an optimization technique (i.e., Genetic Algorithm), a set of input parameters were optimized and employed to simulate the spread of near future fire. As stated by Abdalhaq et al. (2005), this enhanced prediction scheme will accelerate the optimization process of input parameters in real time. Considering the non-uniform distributions of these input parameters along with terrain and time, the above-mentioned scheme has been further modified by coupling meteorological forecast and wind field models. Since the Genetic Algorithm has been applied in the model calibration stage, this new multi-model approach can easily control calibration errors in a certain range without large population sizes. Moreover, the accuracy of fire simulation has been improved (Brun et al., 2014). To deal with dynamic behaviors of input parameters (e.g., wind direction and speed), a statistical system for sorest sire management has been proposed by Bianchini et al. (2010). Based on statistical concepts, this system aggregates all simulated results in all possible scenarios and then statically calculate the burning probability of each area which is applied to simulate the fire spread. Furthermore, by using a data assimilation method (i.e., Sequential Monte Carlo), Xue et al. (2012) developed a new model for fire spread simulation. This model can feed the dynamical real-time data from sensors into simulation process and recursively adjust the system state estimation to improve accuracy of fire simulation results. Meanwhile, in order to overcome the uncertainty of input parameters, Denham et al. (2012) proposed a GA-based dynamic data-driven application system which can automatically adjust highly dynamic input parameters. Results of this research indicated that this system can not only improve the fire simulation performance, but also significantly reduce overall simulation time. By coupling with the evolutionary optimization, Ntinas et al. (2016) developed a data-driven model for fire spread simulation (i.e., parallel fuzzy cellular automaton). Results of this research suggested that this model has the ability of incorporating knowledge from the real observed fires and the propagation rules can be adapted to achieve better simulation accuracy for a specific area.

In summary, most of the models reviewed above mainly focused on the application of data-driven methods to search suitable input parameters (e.g., meteorological and environmental parameters). Moreover, it was hypothesized that, based on historical fire data, a data-driven model can also be applied to create local evolution rules of CA model through a learning procedure. This can simplify the traditional CA modelling approach and improve its adaptability for a specified area.

3. Methodology

Based on fire's driving force data collected in the study area, the major work of this study is to propose a new cellular automaton modelling approach and to validate its performance on simulating the fire spreading. Therefore, the entire operations of the methodology are divided into three sections (see in Fig. 1): (a) Data collection and pre-processing, (b) Modelling approach building, and (c) Model validation. This section mainly introduces the modelling approach building and model validation of the proposed cellular automaton modelling approach. Details of data collection and pre-processing will be described in the next section.

3.1. Modelling approach building: a new cellular automaton

3.1.1. Cell and its state definitions

Traditionally, both square- and hexagonal-lattice can be used to tessellate forest areas. For this work, the square-lattice was selected

tesselate-form

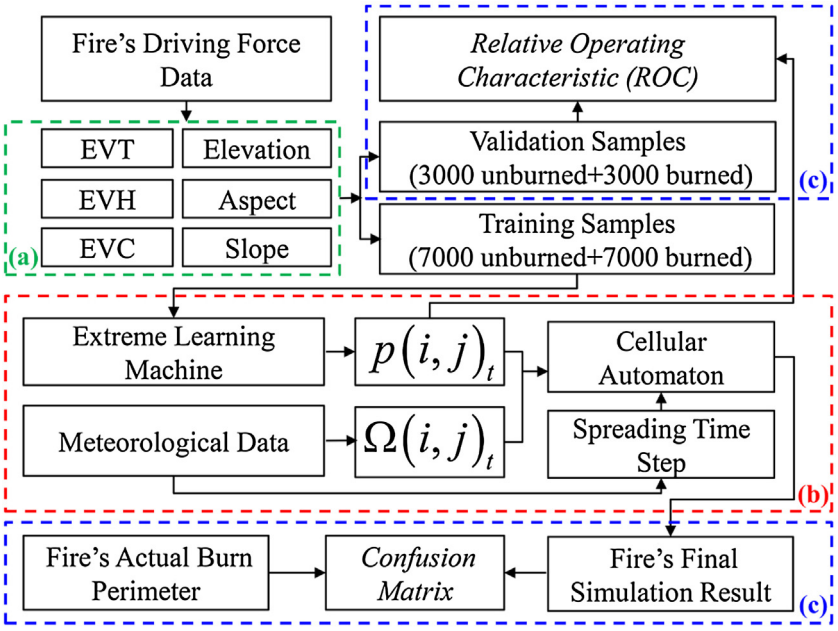

Fig. 1. The flowchart of methodology in this study. (a): Data collection and pre-processing, (b): Modelling approach building, and (c): Model validation.

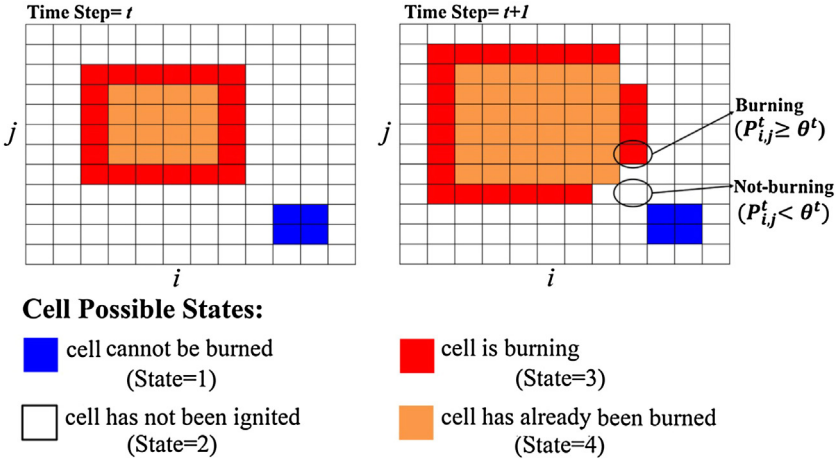

Fig. 2. The basic principle of cellular automaton.

orange->red

and the 2D-regular square grids were used as cells of the CA framework, since this can simplify the calculations and thus considerably reduce computational complexity (Alexandridis et al., 2011). Each square-lattice cell at different discrete time steps can be characterized by the following four possible states (see Fig. 2):

State 1: the cell containing no fuel cannot be burned.

State 2: the cell containing fuel has not been ignited.

State 3: the cell containing fuel is burning.

State 4: the cell containing fuel has already been burned.

3.1.2. Transition rules

In the CA framework, the state of each cell evolves in discrete time steps based on a finite set of local transition rules. In this study, these rules are defined as follow:

3.1.2.1. Rule 1. IF the state of cell (i, j) at discrete time step (t) is unburned; THEN the state of cell (i, j) is unburned at the next discrete time step (t + 1).

This rule means that a cell containing no fuel will not be ignited and thus its state remains as *unburned*.

white->white

3.1.2.2. Rule 2. IF the state of cell (i, j) at discrete time step (t) is burning; THEN the state of cell (i, j) is burned at the next discrete time step (t + 1).

This rule indicates that the state of a burning cell will be updated to be the *burned* state at the next discrete time step.

3.1.2.3. Rule 3. IF the state of cell (i, j) at discrete time step (t) is burned; THEN the state of cell (i, j) is burned at the next discrete time step (t + 1).

orange->orange

This rule implies that the cells that have already been burned cannot be reignited again and thus its state remains as *burned*.

3.1.2.4. Rule 4. IF the state of cell (i, j) at discrete time step (t) is not-ignited and there is one or more than one burning cell in its Moore neighboring cells (i ± 1, j ± 1); THEN the state of cell (i, j) with a higher transition probability (i.e., $P^t_{i,j}$ that measures the likelihood of cell's state transition) will be burning at the next discrete time step (t + 1).

This rule implies that a cell containing combustible fuel will be burning, if one or more than one burning cell in its Moore neigh-

boring cells and its state transition probability (i.e., $P^t_{i,j}$) is higher than a random probability threshold (i.e., θ^t), as shown in Eq. (1):

$$Cell\ (i,j)_{t+1} = \begin{cases} burning & P^t_{i,j} \geq \theta^t \\ unburning & P^t_{i,j} < \theta^t \end{cases} \quad (1)$$

where i, j respectively means the row number and column number of Cell (i, j).

To be specific, the basic principle of above cellular automaton has been shown in Fig. 2.

According to the work of Trunfio (2004), the transition function can be split into two types of components: the internal transformation and the local interaction. Similarly, for each cell (i, j) of this study, its state transition probability can also be expressed as a function of two sub-components, as shown in Eq. (2):

$$P^t_{i,j} = p(i,j)_t * \Omega(i,j)_t \quad (2)$$

where $p(i, j)_t$ is the igniting probability which measures cell's ignited probability influenced by its own factors and $\Omega(i, j)_t$ means neighboring wind effects caused by cell's neighborhoods.

The random probability threshold in Eq. (1) is calculated by following formula (Pei et al., 2015):

$$\theta^t = \beta * 1/\left(1 + \left(-\ln\gamma^t\right)^{\alpha}\right) \quad (3)$$

where γ is a random number between 0 and 1, and the two weight factors (i.e., α and β) can control its effect on random probability threshold.

3.1.3. *Cell igniting probability* p(i, j)$_t$

Similar to the CA framework designed for urban growth simulation, it is assumed that each cell's igniting probability can be determined using a data-driven learning algorithm and fire's driving forces data (e.g., vegetation, wind and topography (Alexandridis et al., 2011)). As an effective and simple machine learning algorithm, ELM was initially proposed for single hidden layer feedforward networks (SLFNs) by Huang et al. (2012), and has already been employed to predict the spread of some spatial phenomenon, e.g., ice loads distributions (Yang et al., 2011). Meanwhile, reported studies suggested that a good generalization performance for ELM could be achieved with much less time costs (Huang, 2015). Therefore, it was adopted and applied in this study to calculate the igniting probability of each cell. The basic concepts of ELM are briefly introduced in the following paragraphs.

For each cell of forest fire, the values of its driving force data are considered as the inputs (i.e., x_i) of ELM model and its igniting probability is considered as the output (i.e., t_i) of ELM model. To be specific, given N distinct samples (x_i, t_i), the goal of ELM estimation is to find a quantitative relationship between $[x_1, x_2, \ldots, x_i]_N$ and $[t_1, t_2, \ldots, t_i]_N$. For the output of an ELM model with M nodes in the hidden layer, it can be represented by Eq. (4):

$$t_i = \sum_{j=1}^{M} \beta_j G_j(x_i) = \sum_{j=1}^{M} \beta_j g_j\left(w_j, x_i, b_j\right) \quad (4)$$

where β_j denotes the output weight of the j-th hidden node, and the $G_j(x_i)$ stands for the output of the j-th hidden node with respect to the i-th x input. The $g_j(\bullet)$ is the activation function mapping samples from the input space to the hidden-layer feature space (Martínez-Martínez et al., 2011). There are different functions available, e.g., Sigmoid, Radial Basis Function, and Fourier Series. The RBF was selected in this study.

Also, Eq. (4) also can be expressed compactly in matrix notation as:

$$T = H \times \beta \quad (5)$$

where B indicates the weights vector of output layer, T represents the ELM outputs, and H refers to the hidden layer output matrix. They can be given by:

$$T = [t_1, t_2, \cdots, t_i]_N \quad (6)$$

$$H = \begin{bmatrix} g(w_1, x_1, b_1) & g(w_2, x_1, b_2) & \cdots g\left(w_j, x_1, b_j\right) \\ g(w_1, x_2, b_1) & g(w_2, x_2, b_2) & \cdots g\left(w_j * x_2, b_j\right) \\ g(w_1, x_i, b_1) & g(w_2, x_i, b_2) & \cdots g\left(w_j * x_i, b_j\right) \end{bmatrix}_{N \times M} \quad (7)$$

$$\beta = \left[\beta_1, \beta_2, \cdots, \beta_j\right]_M \quad (8)$$

Generally, the number of distinct samples is much larger than the number of hidden nodes (i.e., $N >> M$) and the approximation may have small errors (Lan et al., 2010). Thus, Eq. (5) is replaced by:

$$T = H \times \beta + E \quad (9)$$

where $E = [e_1, e_2, \cdots e_i]_N$ represents system residuals. Based on the simple least-squares theory, the cost function of ELM can be defined as:

$$E = \left(T - H \times \beta\right)^T \times \left(T - H \times \beta\right) \quad (10)$$

The ELM estimation can then be transformed to minimize the above cost function (i.e., Eq. (10)). The least-squares solution of ELM is estimated as:

$$\hat{\beta} = H^{\dagger} \times T \quad (11)$$

where $H^{\dagger}$ indicates the Moore-Penrose generalized inverse of hidden layer output matrix H. It can be computed by:

$$H^{\dagger} = \left(H^T \times H\right)^{-1} \quad (12)$$

where H^T refers to the pseudo-inverse matrix.

From the above descriptions, we can find that one of advantages of ELM is that the parameters of its hidden nodes are generated randomly without iterations like some traditional machine learning algorithms (e.g., Back Propagation Neural Network and Support Vector Machine). Since its output weights are analytically determined by computing a simple least-squares solution, another advantage of ELM is that the network's nonlinearities would be fixed without a time-consuming optimization (Lan et al., 2010). Furthermore, ELM can achieve universal approximation capability and classification capability during the learning process of model parameters (Huang et al., 2012; Huang, 2015). Therefore, the trained ELM would be an effective method to calculate the igniting probability of each cell $p(i, j)_t$ in the CA modelling approach. First, distinct samples are selected from historical fires. These samples are then employed to train ELM model (i.e., inputs were driving force values and the output is igniting probability). After the training process is completed, the ELM model is employed to calculate the each cell igniting probability of in the future fire.

3.1.4. *Neighboring wind effect* Ω(i, j)$_t$

Wind is an important factor, which should be considered in CA modelling approach, since its two features (i.e., direction and velocity) can heavily affects the fire spreading. In this study, the wind's effect on cell (i, j) is characterized by the following wind weight matrix:

$$W_{i,j} = \begin{pmatrix} w_{i-1,j-1} & w_{i-1,j} & w_{i-1,j+1} \\ w_{i,j-1} & 1 & w_{i,j+1} \\ w_{i+1,j-1} & w_{i+1,j} & w_{i+1,j+1} \end{pmatrix} \quad (13)$$

If there is no wind blowing on cell (i, j), all weight values of the cells in this 3×3 wind matrix are 1 s (Encinas et al., 2007).

Table 1
The wind weight matrix of neighboring cells.

Wind Direction	$w_{i,\,j-1}$	$w_{i+1,\,j-1}$	$w_{i+1,\,j}$	$w_{i+1,j+1}$	$w_{i,\,j+1}$	$w_{i-1,\,j+1}$	$w_{i-1,\,j}$	$w_{i-1,\,j-1}$
N	1	1	1	1	1	D*sinπ/4	D	D*sinπ/4
S	1	D*sinπ/4	D	D*sinπ/4	1	1	1	1
E	1	1	1	D*sinπ/4	D	D*sinπ/4	1	1
W	D	D*sinπ/4	1	1	1	1	1	D*sinπ/4
S-E	1	1	D*sinπ/4	D	D*sinπ/4	1	1	1
N-W	D*sinπ/4	1	1	1	1	1	D*sinπ/4	D
N-E	1	1	1	1	D*sinπ/4	D	D*sinπ/4	1
S-W	D*sinπ/4	D	D*sinπ/4	1	1	1	1	1

Otherwise, their values would be assigned based on Table 1 (Liu, 2012).

It can be observed in Table 1 that the weights of neighboring cells in the wind blowing direction is much larger in the wind matrix. For example, the values of $w_{i\text{-}1,j+1}$, $w_{i\text{-}1,j}$, and $w_{i\text{-}1,j\text{-}1}$ are larger than the rest of weights, when the wind is blowing from north towards south. Moreover, D is the wind velocity factor, which can also adjust neighboring wind weights.

Then, the neighboring wind effect $\Omega(i,j)_t$ can be computed by:

$$\Omega(i,j)_t = \frac{\sum_{i=1}^{3}\sum_{j=1}^{3} w_{i,j} * C_{i,j}}{\sum_{i=1}^{3}\sum_{j=1}^{3} w_{i,j}} \tag{14}$$

where $C_{i,j}$ is the burning labels. Its value is 1, if the cell is burning. Otherwise, its value is 0.

3.1.5. *Spreading time step* Δt

In the CA modelling approach, the time step (i.e., Δt) is another key parameter, which can significantly influence the spatial pattern of fire spread. With it, the fire spreading time can be converted to the CA modelling approach's iteration times, indicating that we can simulate the growth of fire front contours at different times during the entire firing (Sun et al., 2013). In this study, the heterogeneity of time step in each fire is insignificant, since the obtained input data (e.g., 1 km resolution fuel type data and point-based meteorological data) for calculating time step do not have a fine spatial resolution like cells (i.e., 30 m). Therefore, a fixed time step for each fire was calculated in this study.

As described in Section 2.1.2, a burning cell's state will be updated to be the *burned* state at next discrete time step. This means, within each discrete time step, the fire might travel from one burning cell to its neighbors (Sousa et al., 2012). Thus, Δt can be calculated using the centroid distances between two adjacent cells (i.e., L) and the Rate of Spread (ROS) (Ghisu et al., 2015):

$$\Delta t = \frac{L}{ROS} \tag{15}$$

where the cell size in this study is 30 × 30m, suggesting that the centroid distance L for adjacent cell is 30 m. In particular, for simplifying the CA modelling process, we do not distinguish between adjacent and diagonal cells in this study. Therefore, all centroid distances for adjacent and diagonal cells were approximately equal to 30 m. For ROS, it is predicted by using the spread component of national fire danger rating system (NFDRS) calculator. Based on input data (e.g., fuel modelling approach characteristics, live fuel moistures, the 0–3 in. dead fuel moisture, wind speed and slope class), this calculator can generate a fixed ROS for each fire (National Fire and Aviation Management, 2015).

3.2. *Model validation*

3.2.1. *ROC*

Before applying the trained ELM model to calculate the igniting probabilities for all cells across the entire study area, its accuracy evaluation is required. In this study, the Relative Operating Characteristic (ROC) method is used, since it can quantitatively measure the accuracy of a probability prediction compared to the observed events that actually occurred (Fang et al., 2005). For conducting the ROC analysis, the validation sample data are extracted over forest area using stratified simple random sampling methods. Then, according to a series of igniting probability threshold levels (i.e., 0.1–1), these sample data can be reclassified into 100 subdivisions (Park et al., 2011). For each generated subdivision, the true-positive proportion and false-positive proportion is calculated (Wu et al., 2009). Based on these proportion values, the ROC curve is plotted and the ROC statistics (i.e., Area under Curve-AUC) is then computed. If the predicting probability has no effect on fire igniting discrimination, the corresponding AUC value will be 0.5 (Fang et al., 2005). A value between 0.7–0.9 means the predicting igniting probability has a reliable performance while a value above 0.9 or under 0.7 indicates best or poor performance, respectively (Wu et al., 2009).

stratified->to divide into classes

3.2.2. *Confusion matrix*

After the simulation process, the quantitative comparison between the final simulation results and the real burned area for each fire is conducted. In most cases, the accuracy of CA-based fire simulating modelling approach is evaluated using a visual inspection of the final simulation results and the real fire spread (Alexandridis et al., 2011). In this study, the confusion matrix, i.e., a standard accuracy assessment for remote sensing image classifications is applied. For details, as far as the final burned area is predicted, its boundary is overlaid with fire's real burned perimeter. The confusion matrix is calculated and the five quantitative measurements (i.e., burned actual-burned predicted (%), burned actual-not burned predicted (%), not burned actual-burned predicted (%), burned actual area (km^2), and burned predicted area (km^2)) are recorded.

4. Materials

4.1. *Study areas*

Five fires, located in the west of United States, were simulated in this study (see Fig. 3). Four of the fires (i.e., Coal Seam Fire, Spring Creek Fire, Big Elk Fire and Bear Fire) are largest wildfires in the Colorado history and the remaining one (i.e., Mustang Fire) occurred in the northeastern Utah State.

The Coal Seam Fire started on June 08, 2002 and ended on June 29, 2002. It was used to generate the samples for ELM training. This fire is located at the Glenwood Springs area, where the humidity is relative lower all the year round with a semi-arid climate. This area's annual rainfall averages 381–432 mm in the valley and can

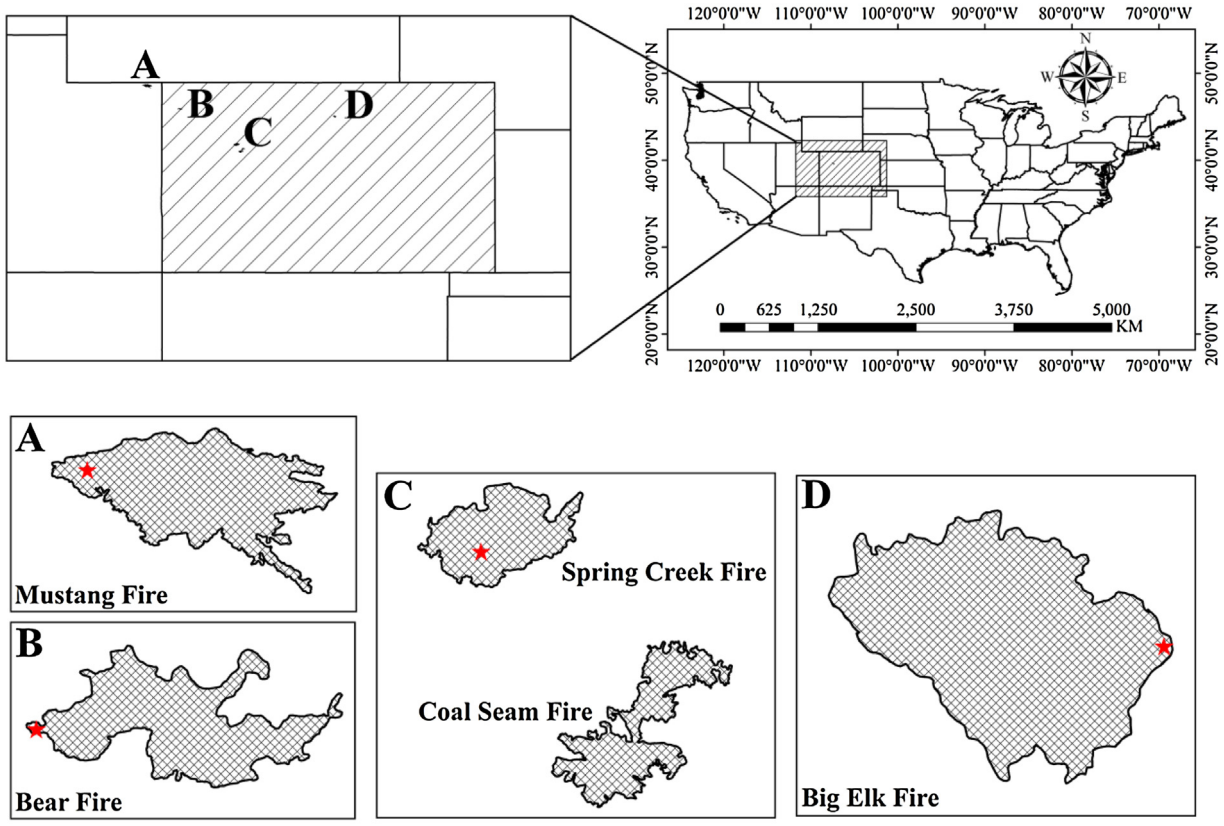

Fig. 3. Study areas (the red star shows the starting point of each fire). (For interpretation of the references to colour in this figure legend, the reader is referred to the web version of this article.)

rise up to 965 mm in high height area (Cannon et al., 2003). The crucial rain falls during the winter frontal storms or the summer convective thunderstorms (Cannon et al., 2003). Meanwhile, the average high temperature of this area for the winter range 30–40 °C at the bottom of the valley and 80–90 °C during the summer season. The elevation of burned area ranges from 1714 to 3190 m. The major vegetation types in this area are piñon-juniper woodlands, mountain shrublands, and aspen, Douglas fir, and spruce-fir forests.

The Spring Creek Fire was the first fire that we selected to simulate in this study. It is located at 12.87 km away from the north of the New Castle area, in which the average annual precipitation is 410 mm, the annual average humidity is 77.08%, and the annual average temperature is 8 °C. Its major vegetation types are Engelmann spruce-subalpine fir, white fir, big sagebrush, aspen, Douglas fir and serviceberry. On June 22, 2002, the Spring Creek Fire was started by a lightning and then spread south in the next few days. After that, the fire spread towards the southwest under the wind function and was finally brought under control on July 05, 2002. According to statistics, this fire killed 2 people and led to the loss of more than 3,985,000 dollars. The total burned area is about 47.22 km^2 and is mainly located at elevation between 2000 and 3469 m.

The Big Elk Fire was selected as the second fire for spreading simulation in this study. This fire lies in some 14.48 km south east from the Estes Park area, where the average annual precipitation is 415 mm, annual average temperature is 5 °C, and annual average humidity is 81.89%. This area is mainly covered with aspen, lodgepole pine, white fir, Douglas fir, juniper-pinyon pine, chokecherry, serviceberry, ponderosa pine and rose. On July 17, 2002, the Big Elk Fire was started by human and moved 5 km to the northwest. Then, its behavior varied with the impact of various driving factors. By July 22, 2002, this fire was controlled, which resulted in 3 deaths and 1,080,000 dollars in damage. Its final burned area is about 17.59 km^2 and ranges from 2064 to 2828 m elevations.

The Mustang Fire was the third fire which we simulated. It is near the Vernal area, where the average annual precipitation is 234 mm, the annual average temperature 6 °C, and the annual average humidity is 78.36%. The major vegetation types are saltbush-greasewood, juniper-pinyon pine, big sagebrush, bluebunch wheatgrass, and salt desert shrub. This fire was caused by human on June 30, 2002 and extended over the Dutch John Mountain and to the south and east of the ridge (Jackson et al., 2005). By July 05, 2002, the extending of this fire was ended and more than 83.39 km^2 forested areas were destroyed. This burned area elevation ranges from 1669 to 2808 m.

The Bear Fire was the last fire analyzed in this study. It also was one of the largest wildfires in Colorado history, which was located in the Dinosaur National Monument area. In this area, the annual precipitation is lower than 300 mm and the major vegetation are pinyon-juniper, big sagebrush, ponderosa pine, rocky mountain lower montane-foothill, curl-leaf mountain mahogany, dry-mesic montane mixed conifer, and so on. The fire started on June 27, 2002 and then extended to eastern. By July 8, 2002, it was out and caused about 20.16 km^2 areas damage. The elevation of the burned area ranges from 1647 to 2440 m.

4.2. Data and pre-processing

This section describes the data used in this study as well as the steps we took to pre-process the data. The fire's driving force data were collected from the LANDFIRE, in which some landscape scale geo-spatial products for fire research have been made available (LANDFIRE, 2015). Based on some previous studies for fire spreading (Alexandridis et al., 2008; Alexandridis et al., 2011), two types of

variables were selected: existing vegetation data and topographic data. Existing vegetation data (i.e., Existing Vegetation Type (EVT), Existing Vegetation Cover (EVC), and Existing Vegetation Height (EVH)) were downloaded from the 2001 version product of the LANDFIRE program (i.e., the LF 2001: Refresh-LF_1.0.5), which was mapped using the 30-m resolution remote sensing images acquired in 2001. This can ensure that the pre-fire vegetation condition for each fire simulated in the study is more convincing, since all fires were started in 2002. The topographic data (i.e., Aspect, Elevation and Slope) also were downloaded from the LANDFIRE program. They were derived from the National Elevation Dataset (NED) with 1 arc-second high resolution (approx. 30 m) and can be used in modelling approaches to predict wildland fire behavior and effects (LANDFIRE, 2015).

For each distinct sample, its driving force values were considered as the input (i.e., x_i) of ELM model, and its igniting probability (i.e., t_i) was considered as the output of ELM model. If the distinct sample was extracted from unburned area, its igniting probability was assigned as 0. Otherwise, its igniting probability (i.e., t_i) was assigned as 1 if it was extracted from burned area. In this study, about 14000 distinct samples with input values and igniting probabilities were randomly extracted from the Coal Seam Fire: 7000 over unburned areas and 7000 over burned areas. These distinct samples were then used to train the ELM model. After that, using the driving force values of validation samples for each fire as the input of trained ELM, we calculated each sample's igniting probability and applied it to evaluate the ELM's performance. Specifically, for each fire in this study, the total number of validation samples was about 6000, including 3000 from burned areas and 3000 from unburned areas.

Meanwhile, as an important factor affecting the fire spread behavior, meteorological data were collected from the RAWS USA Climate Archive, which was provided by the Western Regional Climate Center (WRCC, 2015). They were used as the inputs of neighboring wind effect and spreading time step. In this study, based on each fire's location, the nearest weather station was selected and its weather observing values during the fire spreading period were averaged to represent the mean weather condition. The detail meteorological information can be found in Table 2.

Also, the fire occurrence data for setting the starting point of the CA modelling approach were collected from the Fire and Aviation Management Web Application (FAMWEB, 2015). These data record the original starting location of each fire event. Moreover, burned perimeters used for the accuracy quantitative evaluation were downloaded from the Monitoring Trends in Burn Severity program (MTBS, 2013).

5. Results and discussion

5.1. The accuracy evaluation of ELM

The ROC curve for each fire is shown in Fig. 4. Its AUC value illustrates how well the calculated igniting probability discriminate each cell's ignition. It can be observed that the ROC curve for the Coal Seam Fire has a larger AUC value (i.e., AUC = 0.80) than the reliable performance threshold value (i.e., AUC = 0.70), which indicates that the ELM trained from the distinct sample of the Coal Seam Fire has a reliable performance on calculating the igniting probability over the rest burned areas of this fire.

Additionally, when we used this trained ELM to predict the igniting probability of coming fires broke out in the neighborhood, the AUC values for other forest fires (i.e., Spring Creek Fire, Big Elk Fire, Mustang Fire and Bear Fire) were 0.69, 0.74, 0.70, and 0.72, respectively. From this result (i.e., almost all AUCs of these fires are larger than 0.70), we can say that the trained ELM also had a credible precision when it was used to predict the igniting probability of future fires broke out in the neighborhood.

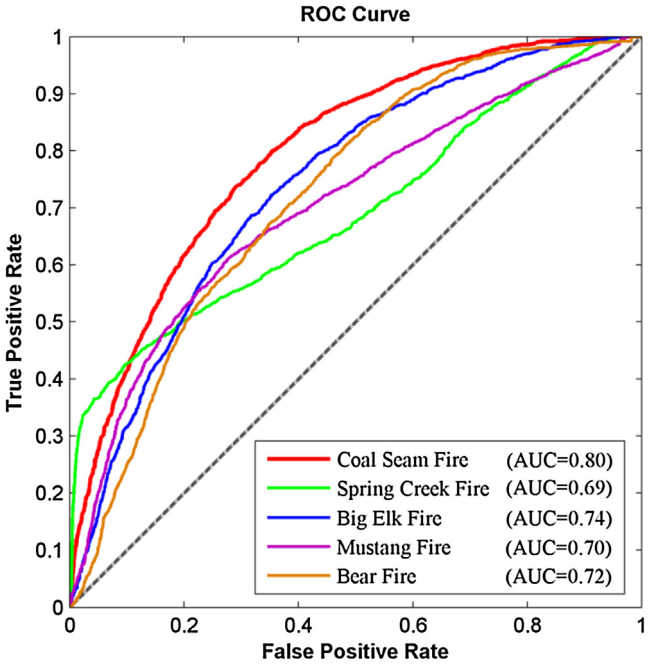

Fig. 4. ROC curves comparison among different forest fires. The dashed line indicates igniting probability is completely random and has no effect on fire igniting discrimination (i.e., its AUC value is 0.5).

In most cases, each cell's igniting probability of CA modelling approach was calculated using the fire physical velocity modelling approach, e.g., Rothermel's and Wang's modelling approach. In general, these modelling approaches are complex and generally need to be adjusted to make it more suitable for a specified fire simulation, which means that intensive preliminary researches and additional field experiments are needed. Unlike them, the machine learning method (i.e., the ELM in this study) was conducted in this study to calculate the cell's igniting probability. Only some training samples collected from neighborhood fires are required. Furthermore, the results in Fig. 4 confirm the fact that the ELM performs effectively in predicting the igniting probability of each cell. Results from other research fields, e.g., the land use/cover growth modelling (Li and Yeh, 2002), also support this fact.

Additionally, the results in Fig. 4 also show that, using neighborhood historic data, the ELM can predict the cell's igniting probability of future fire. This means that the proposed CA modelling approach of this study can predict each process of further fire spreading using the training data collected in the historic neighborhood fires, rather than just simulate a fire that already happened.

5.2. Wind sensitivity analysis

The wind is a critical factor affecting fire spreading patterns. This study investigated the effects of the wind parameters (i.e., direction and velocity), which is shown in Fig. 5. Fig. 5(a)–(h) show that the fire spreads along the downwind direction, in the case that the wind velocity remains unchanged (i.e., D = 4). This means that the proposed CA modelling approach can effectively simulate the effect of wind's direction on fire spreading behaviors. Meanwhile, Fig. 5(i)–(l) display that, under the circumstance that the wind direction is stable (i.e., West), the wind velocity is another parameter affecting fire spreading. The higher wind velocity leads to the smaller spreading angle in the windward direction. This simulation is quite consistent with the real situation. Therefore, the proposed

Table 2
The fire and detail meteorological information during fire spreading.

Fire Name	Initial Date	Controlled Date	Burned Area (km^2)	Average Wind Speed (m/s)	Average Air Temperature (°C)	Average Relative Humidity (%)
Coal Seam Fire	06/08/2002	06/29/2002	48.58	4.78	18.53	23.14
Spring Creek Fire	06/22/2002	07/05/2002	47.22	5.14	19.79	28.57
Big Elk Fire	07/17/2002	07/22/2002	17.59	1.22	19.70	42.00
Mustang Fire	06/30/2002	07/05/2002	83.39	1.11	24.75	16.83
Bear Fire	06/27/2002	07/08/2002	20.16	2.15	27.48	17.25

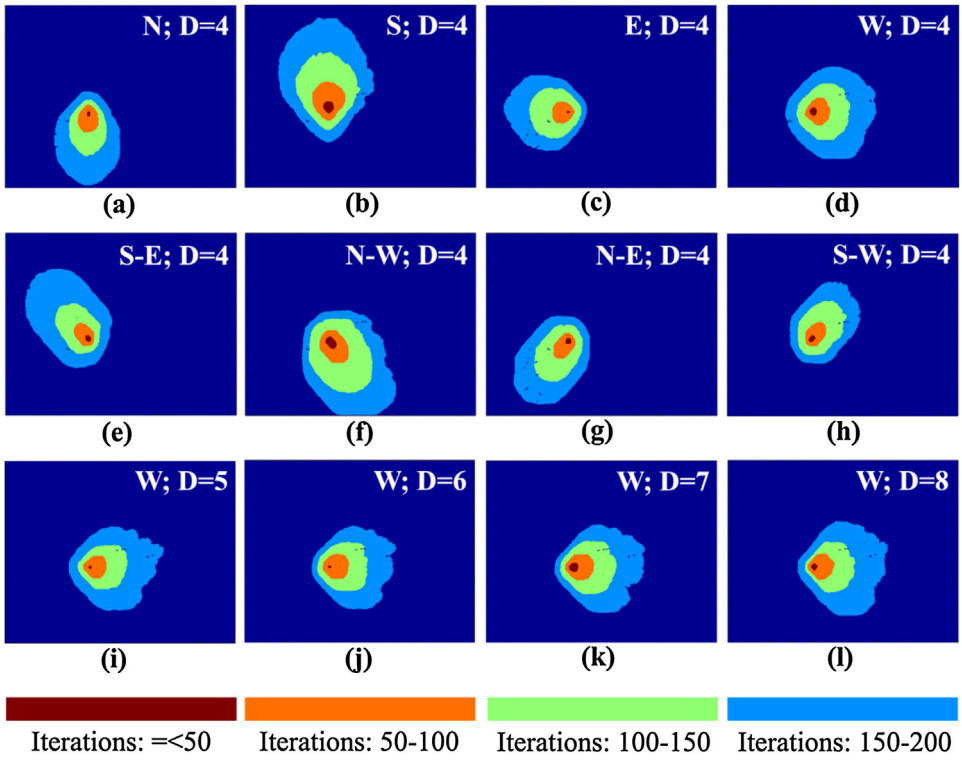

Fig. 5. The wind sensitivity analysis results of the Spring Creek Fire.

CA modelling approach is capable of describing the impact of wind velocity on fire spreading pattern.

It is important to note that, similar to wind parameters, terrain slope also has a directional effect on fire spreading. However, this directional effect has not been considered in the proposed model for simplifying model building process. Instead, the indirect influence of terrain slope on fire spreading has been incorporated in CA model through calculating the transition probability of each cell.

5.3. Accuracy evaluation of simulation results for each fire

Fig. 6 presents the simulation results of the spreading process of four fires and their comparison with the fire's real burn perimeter. For each fire, its spreading direction simulated using the proposed CA modelling approach shows a good agreement with the true direction displayed by the actual burn perimeter which was collected from the official sources. From a quantitative perspective, Table 3 shows the Burned Actual-Burned Predicted percentage varies between 58.45% and 82.08%, which are better than that of the reported studies (67.7%) (Alexandridis et al., 2011) and thus indicates that the final simulation result for each fire is close to the real one. In particular, the simulation results showed by green box are consistent with the actual of burned areas (Fig. 6(c)). This is because the cells in green box contain no fuel, which indicates that the proposed CA modelling approach successfully simulated the condition that the fire bypassed the incombustible materials during the spreading process.

However, Fig. 6 shows that there are some discrepancies between each fire's simulation result and its actual burn perimeter. For the Spring Creek Fire (see Fig. 6(a)) and the Big Elk Fire (see Fig. 6(b)), we can see that the significant deviation from simulations and final burned area is located in areas represented by the red box. According to the official report, the spotting fire appeared in these areas. This leads to the larger spreading pattern differences under the affection of variable meteorological factors. Also, for the river in the Bear Fire (showed in the red box of Fig. 6(d)), we can find that the fire spreading still crosses the river reaching the other side of the river, although igniting probabilities of cells at the river locations are 0s. This is a significant disadvantage of the proposed CA modelling approach, which needs to be further studied and improved.

In practice, the simulation of the fire's spread pattern cannot exactly match with the actual fire behavior, since not all fire records can meet the necessary demands for fire simulation in general, e.g., the collected vegetation and meteorological data are not often complete (Trunfio, 2004). To take the meteorological factors (e.g., wind, air temperature, and relative humidity), for example, the accuracy of their real-time observing data are of extreme importance for precisely simulating the fire's spreading process. Moreover, these real-time meteorological data generally are observed at sparse

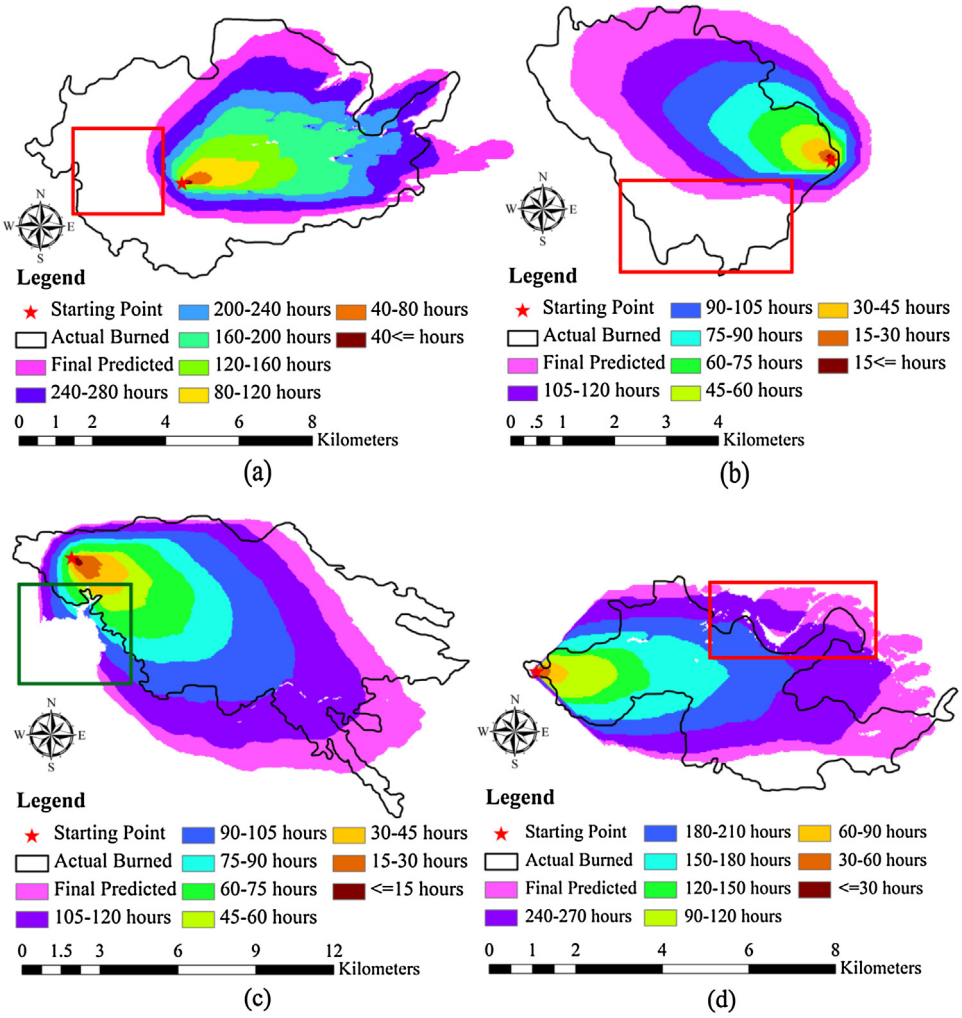

Fig. 6. Comparison between simulation results and actual burn perimeter. (a): Spring Creek Fire, (b): Big Elk Fire, (c): Mustang Fire, and (d): Bear Fire.

Table 3
Quantitative comparison between simulation results and actual burn.

State	Simulating Performance of Each Fire			
	Spring Creek Fire	Big Elk Fire	Mustang Fire	Bear Fire
Burned Actual-Burned Predicted (%)	58.45	68.86	82.08	81.79
Burned Actual-Not Burned Predicted (%)	41.55	31.14	17.92	18.21
Not Burned Actual-Burned Predicted (%)	2.91	8.99	14.9	19.03
Burned Actual Area (km^2)	47.22	17.59	83.39	20.16
Burned Predicted Area (km^2)	31.58	16.13	97.57	29.29

Table 4
Optimized parameters of proposed model for each simulated fire.

Parameters	Simulated Fire			
	Spring Creek Fire	Big Elk Fire	Mustang Fire	Bear Fire
α	1.7	2.3	2.1	2.3
β	2.0	4.1	2.2	3.4
D	9	3	3	5

monitoring sites, meaning accurate surface-based meteorological data cannot be easily obtained. This will lead to the discrepancy between each fire's simulation result and its actual burn perimeter, since the meteorological condition at each cell is different in the fire combustion process.

In general, optimized parameters of CA modelling approach (i.e., α, β, and D in Table 4) have local adaptability since environmental and meteorological factors (e.g., wind's direction and velocity) are changeable for a specific fire. From a practical point of view, an iterative optimization procedure would be a more effective way to determine these model's parameters (Alexandridis et al., 2011), since it could improve CA model's adaptability for a specified area without investigating the influence of these local parameters on modelling results. Each pair of possible values (i.e., α, β, and D) was tested at each iteration in this study and the set of parameters with the best simulated performance were selected. This might be a time consuming process. However, according to the reported studies (Ntinas et al., 2016; Denham et al., 2012), some intelligent algorithms (e.g., Genetic Algorithm) can be applied to accelerate the determination process of optimal parameters in our future research.

It should be noted that, similar to previous studies on probabilistic CA model for spread simulation of forest fires (Alexandridis

et al., 2011), a strong constraint has been introduced into the proposed model, i.e., the fire in a cell lasts for just one time step. This design may make the internal process of fire spread in a cell unclear. However, since state switching of each cell is determined through the accumulation of igniting probability like that of traditional ROS-based CA models, the effect of this constraint on whole simulation results is insignificant. Meanwhile, as a probabilistic model, the performance of this proposed model would be affected by the variety of random seeds. After some repeated tests, it can be found that this effect will be limited due to the number of random seeds is large enough in this study (i.e., 14000 training samples and 6000 validation samples for each fire). Meanwhile, the ROC method provides additional measurement to evaluate the accuracy of probability prediction, which can further ensure the performance of proposed model.

6. Conclusions

For quickly designing risk management and effectively implementing suppression policies, it is widely needed to simulate the fire spreading process quantitatively. In this study, we proposed a new cellular automaton modelling approach that integrates the traditional forest fire CA framework with the ELM. The analysis was conducted in five selected historic fires located at the west of United States. Results indicate that the ELM performed well in predicting each cell's igniting probability, the proposed method can effectively describe impact of wind velocity on fire spreading pattern, and the simulation accuracy (i.e., the Burned Actual-Burned Predicted is between 58.45 and 82.08%) is reliable. We can conclude that the proposed modelling approach is easily applied and effectively simulated the fire behavior.

Acknowledgments

This work has been funded by the National Science Foundation of China (No. 41171326, 40771198), the Fundamental Research Funds for the Central Universities of Central South University (No. 2015zzts070), and the Project Supported by the Scientific Research Foundation of CUIT. The authors would like to acknowledge the U.S. Forest Service Remote Sensing Applications Center, the U.S. Geological Survey National Center for Earth Resources Observation and Science, the USDA Forest Service's Fire and Aviation Management, the U.S. Western Regional Climate Center, the U.S. Department of Agriculture Forest Service, and the U.S. Department of the Interior for making their data available. We wish to thank the editor and anonymous reviewers for their thoughtful and helpful comments.

References

Abdalhaq, B., Cortés, A., Margalef, T., Luque, E., 2005. Enhancing wildland fire prediction on cluster systems applying evolutionary optimization techniques. Fut. Gener. Comput. Syst. 21, 61–67.

Albinet, G., Searby, G., Stauffer, D., 1986. Fire propagation in a 2-D random medium. J. Phys. 47, 1–7.

Alexandridis, A., Vakalis, D., Siettos, C.I., Bafas, G.V., 2008. A cellular automata model for forest fire spread prediction: the case of the wildfire that swept through Spetses Island in 1990. Appl. Math. Comput. 204, 191–201.

Alexandridis, A., Russo, L., Vakalis, D., Bafas, G., Siettos, C., 2011. Wildland fire spread modelling using cellular automata: evolution in large-scale spatially heterogeneous environments under fire suppression tactics. Int. J. Wildland Fire 20, 633–647.

Bianchini, G., Denham, M., Cortés, A., Margalef, T., Luque, E., 2010. Wildland fire growth prediction method based on multiple overlapping solution. J. Comput. Sci. 1, 229–237.

Brun, C., Margalef, T., Cortés, A., Sikora, A., 2014. Enhancing multi-model forest fire spread prediction by exploiting multi-core parallelism. J. Supercomput. 70, 721–732.

Cannon, S.H., Gartner, J.E., Holland-Sears, A., Thurston, B.M., Gleason, J.A., 2003. Debris-flow response of basins burned by the 2002 Coal Seam and Missionary Ridge fires, Colorado. In: Boyer, D.D., Santi, P.M., Rogers, W.P. (Eds.), Engineering Geology in Colorado-contributions, Trends, and Case Histories. AEG Special Publication 15. Colorado Geological Survey Special Publication.

Chang, Y., Zhu, Z., Feng, Y., Li, Y., Bu, R., Hu, Y., 2016. The spatial variation in forest burn severity in Heilongjiang Province, China. Nat. Hazards 81, 981–1001.

Clarke, K.C., Gaydos, L.J., 1998. Loose-coupling a cellular automaton model and GIS:long-term urban growth prediction for San Francisco and Washington/Baltimore. Int. J. Geogr. Inf. Sci. 12, 699–714.

Collin, A., Bernardin, D., Sero-Guillaume, O., 2011. A physical-based cellular automaton model for forest-fire propagation. Combust. Sci. Technol. 183, 347–369.

Denham, M., Wendt, K., Bianchini, G., Cortés, A., Margalef, T., 2012. Dynamic data-driven genetic algorithm for forest fire spread prediction. J. Comput. Sci. 3, 398–404.

Encinas, A.H.a., Encinas, L.H.a., White, S.H., del Rey, A.M.i., S'anchez, G.R.i., 2007. Simulation of forest fire fronts using cellular automata. Adv. Eng. Softw. 38, 372–378.

FAMWEB, 2015. Fire & Weather Data, 14 December, 2015 http://fam.nwcg.gov/fam-web/weatherfirecd/.

Fang, S., Gertner, G.Z., Sun, Z., Anderson, A.A., 2005. The impact of interactions in spatial simulation of the dynamics of urban sprawl. Landsc. Urban Plan. 73, 294–306.

Ghisu, T., Arca, B., Pellizzaro, G., Duce, P., 2015. An optimal Cellular Automata algorithm for simulating wildfire spread. Environ. Modell. Softw. 71, 1–14.

Gonçalves, P., Diogo, P., 1994. Geographic information systems and cellular automata: A new approach to forest fire simulation. In: Proceedings of The European Conference on Geographical Information Systems (EGIS 94), Paris, France, pp. 702–712.

Hernández Encinas, A., Hernández Encinas, L., Hoya White, S., Martín del Rey, A., Rodríguez Sanchez, G., 2007. Simulation of forest fire fronts using cellular automata. Adv. Eng. Softw. 38, 372–378.

Hogeweg, P., 1988. Cellular automata as a paradigm for ecological modeling. Appl. Math. Comput. 27, 81–100.

Huang, G., Zhou, H., Ding, X., Zhang, R., 2012. Extreme learning machine for regression and multiclass classification. IEEE Trans. Syst. Man Cybern. Part B: Cybern. 42, 513–529.

Huang, G., 2015. What are extreme learning machines?: Filling the gap between Frank Rosenblatt's dream and John von Neumann's puzzle. Cognit. Comput. 7, 263–278.

Jackson, S.T., Betancourt, J.L., Lyford, M.E., Gray, S.T., Rylander, K.A., 2005. A 40,000-year woodrat-midden record of vegetational and biogeographical dynamics in north-eastern Utah, USA. J. Biogeogr. 32, 1085–1106.

Karafyllidis, I., Thanailakis, A., 1997. A model for predicting forest fire spreading using cellular automata. Ecol. Model. 99, 87–97.

LANDFIRE, 2015. Vegetation Products, 10 December, 2015 http://www.landfire.gov/.

Lan, Y., Soh, Y.C., Huang, G.-B., 2010. Two-stage extreme learning machine for regression. Neurocomputing 73, 3028–3038.

Li, X., Liu, X., 2006. An extended cellular automaton using case-based reasoning for simulating urban development in a large complex region. Int. J. Geogr. Inf. Sci. 20, 1109–1136.

Li, X., Yeh, A.G.-O., 2002. Neural-network-based cellular automata for simulating multiple land use changes using GIS. Int. J. Geogr. Inf. Sci. 16, 323–343.

Liu, C., 2012. The Study of Forest Fire Spread Model Based Cellular Automata and Simulation. Dalian University of Technology, Dalian.

MTBS, 2013. Monitoring Trends in Burn Severity, 5 December, 2013 http://mtbs.gov/index.html.

Martínez-Martínez, J.M., Escandell-Montero, P., Soria-Olivas, E., Martín-Guerrero, J.D., Magdalena-Benedito, R., Gómez-Sanchis, J., 2011. Regularized extreme learning machine for regression problems. Neurocomputing 74, 3716–3721.

Meyer, D.A., 1996. From quantum cellular automata to quantum lattice gases. J. Stat. Phys. 85, 551–574.

National Fire and Aviation Management, 2015. WIMS User Guide (12 December, 2015) https://fam.nwcg.gov/fam-web/pocketcards/wims_ug_final/wims_ug.html.

Niessen, W.V., Blumen, A., 1988. Dynamic simulation of forest fires. Can. J. For. Res. 18, 807–814.

Ntinas, V.G., Moutafis, B.E., Trunfio, G.A., Sirakoulis, G.C., 2016. Parallel fuzzy cellular automata for data-driven simulation of wildfire spreading. J. Comput. Sci., http://dx.doi.org/10.1016/j.jocs.2016.08.003.

Park, S., Jeon, S., Kim, S., Choi, C., 2011. Prediction and comparison of urban growth by land suitability index mapping using GIS and RS in South Korea. Landsc. Urban Plan. 99, 104–114.

Pei, F., Xia, L., Xiaoping, L., Gengrui, X., 2015. Dynamic simulation of urban expansion and their effects on net primary productivity: a scenario analysis of Guangdong province in China. J. Geoinf. Sci. 17, 469–477.

Quintano, C., Fernández-Manso, A., Roberts, D.A., 2013. Multiple Endmember Spectral Mixture Analysis (MESMA) to map burn severity levels from Landsat images in Mediterranean countries. Remote Sens. Environ. 136, 76–88.

Rienow, A., Goetzke, R., 2015. Supporting SLEUTH–Enhancing a cellular automaton with support vector machines for urban growth modeling. Comput. Environ. Urban Syst. 49, 66–81.

Russo, L., Russo, P., Vakalisc, D., Siettos, C., 2014. Detecting weak points of wildland fire spread:a cellular automata model risk assessment simulation approach. Chem. Eng. Trans. 36, 253–258.

Sousa, F.A., Dos Reis, R.J.N., Pereira, J.C.F., 2012. Simulation of surface fire fronts using fireLib and GPUs. Environ. Modell. Softw. 38, 167–177.

Sullivan, A.L., 2009a. Wildland surface fire spread modelling, 1990–2007. 1: physical and quasi-physical models. Int. J. Wildland Fire 18, 349–368.
Sullivan, A.L., 2009b. Wildland surface fire spread modelling, 1990–2007. 2: empirical and quasi-empirical models. Int. J. Wildland Fire 18, 369–386.
Sullivan, A.L., 2009c. Wildland surface fire spread modelling, 1990–2007. 3: simulation and mathematical analogue models. Int. J. Wildland Fire 18, 387–403.
Sun, T., Zhang, L., Chen, W., Tang, X., Qin, Q., 2013. Mountains forest fire spread simulator based on geo-cellular automaton combined with Wang Zhengfei velocity model. IEEE J. Sel. Top. Appl. Earth Observ. Remote Sens. 6, 1971–1987.
Trunfio, G.A., 2004. Predicting wildfire spreading through a hexagonal cellular automata model. In: P.M.A, Sloot, B.C., Hoekstra, A.G. (Eds.), Cellular Automata. Springer, Berlin, Heidelberg, pp. 385–394.
von Neumann, J., 1966. Theory of Self-Reproducing Automata. University of Illinois Press, pp. 388.
WRCC, 2015. RAWS USA Climate Archive, 9 May, 2015 http://www.raws.dri.edu/.
Wang, Z.F., 1992. General forest fire weather ranks system. J. Nat. Disasters 1, 39–45.
White, S.H., del Rey, A.M.i., S'anchez, G.R.i., 2007. Modeling epidemics using cellular automata. Appl. Math. Comput. 186, 193–202.
Wu, X., Hu, Y., He, H.S., Bu, R., Onsted, J., Xi, F., 2009. Performance evaluation of the SLEUTH model in the Shenyang metropolitan area of northeastern China. Environ. Model. Assess. 14, 221–230.
Xue, H., Gu, F., Hu, X., 2012. Data assimilation using sequential monte carlo methods in wildfire spread simulation. ACM Trans. Model. Comput. Simul. 22 (23), 1–25 (25).
Yang, H., Xu, W., Zhao, J., Wang, D., Dong, Z., 2011. Predicting the probability of ice storm damages to electricity transmission facilities based on ELM and Copula function. Neurocomputing 74, 2573–2581.
Zhang, Y., Feng, Z., Han, T., Wu, L., Li, K., Duan, X., 2004. Simulating wildfire spreading processes in a spatially heterogeneous landscapes using an improved cellular automaton model, IGARSS' 04. In: Proceedings of the 2004 IEEE International, IEEE, pp. 3371–3374.
Zheng, Z., Zeng, Y., Li, S., Huang, W., 2016. A new burn severity index based on land surface temperature and enhanced vegetation index. Int. J. Appl. Earth Obs. Geoinf. 45, 84–94.